

# Reduction of Ringing Losses in Flyback Converter by Using the RC-RCD Clamp Circuit

UDK 621.376.5:621.314.6  
 IFAC 4.3.1

Original scientific paper

Flyback converter is one of the most popular DC-DC converters for low power supply. Due to the transformer leakage inductance the converter suffers from the voltage spikes, which can be »controlled« by the dissipative RCD or non-dissipative LCD clamp circuits. Both of the clamp circuits consist of the diode. The diode reverse recovery charge causes the oscillation, which results in additional dissipation of the clamp circuitry. This paper describes this ringing phenomenon and the use of an RC-RCD clamp circuit for damping the clamp-diode's oscillation. This clamp circuit is capable for improving a flyback converter's power ratio.

**Key words:** clamp circuit, flyback converter, ringing losses

## 1 INTRODUCTION

The large surge voltage arises during transistor turn-off in the switching power converters with transformer. The surge generation is due to transformer leakage inductance, and an RC clamp circuit is usually inserted to absorb the energy stored in the inductance and to suppress the surge voltage. From the viewpoint of minimizing the dissipative energy in the clamp circuit, the optimization of the RC clamp has been reported in [1]. Due to converters efficiency the non-dissipative clamp circuit was proposed in [2] where the authors instead of the conventional RC clamp introduced the non-dissipative LC clamp circuit. Both of these principles do not consider the diode reverse recovery effect which causes the well known oscillation in surge voltages during transistor turn-off.

This paper explores the reverse recovery diode effect on the clamp circuits. The diode capacitance  $C_{rr}$  (reverse recovery charge is stored in this capacitor) and leakage inductance  $L_\ell$  establish the series resonant tank circuit when the diode is turned-off. The high frequency oscillation appears. This undesirable diode power dissipation in the reverse region can be suppressed by the introduction of an RC-RCD structured clamp circuit. Consequently, the power ratio and the EMI of the converter can be improved. This process was investigated by simulation, and verified experimentally.

## 2 DISSIPATIVE RCD CLAMP CIRCUITS

The operation of most transformer-isolated converters can be adequately understood by modeling the transformer with a simple equivalent circuit consisting of an ideal transformer, a leakage and magnetizing inductances (Figure 1). The magnetizing inductance must then follow all the usual rules for inductors. This means that the inductor

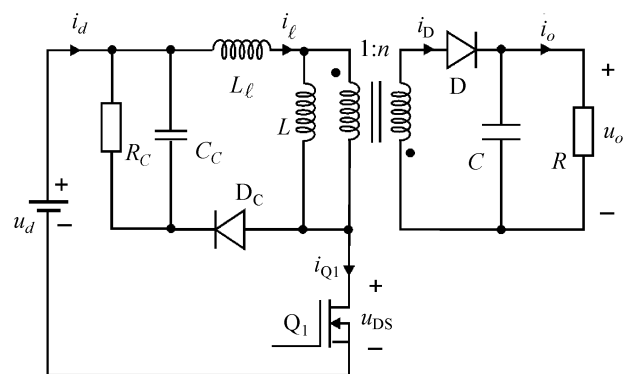


Fig. 1 Dissipative RCD clamp circuit in fly-back converter

must be designed according to the current ripple requirements. In order to avoid the inductor saturation, the transformer must be designed with air gap, consequently, the leakage inductance ( $L_\ell$ ) is not negligible.

The leakage inductance is effectively connected in series with transistor  $Q_1$ . When transistor switches off, it interrupts current flowing through  $L_\ell$ . This action induces voltage spike according to:

$$u_\ell(t) = L_\ell \frac{di_\ell}{dt}. \quad (1)$$

The converter in Figure 1 has been tested for output load of 50 W. The transistor voltage wave-shape during the switching off interval without clamp circuit is shown in Figure 2 (a). If the peak magnitude of the voltage spike exceeds the voltage rating of the transistor, than transistor fails. The voltage spike can be supervised by protection clamp circuit [5].

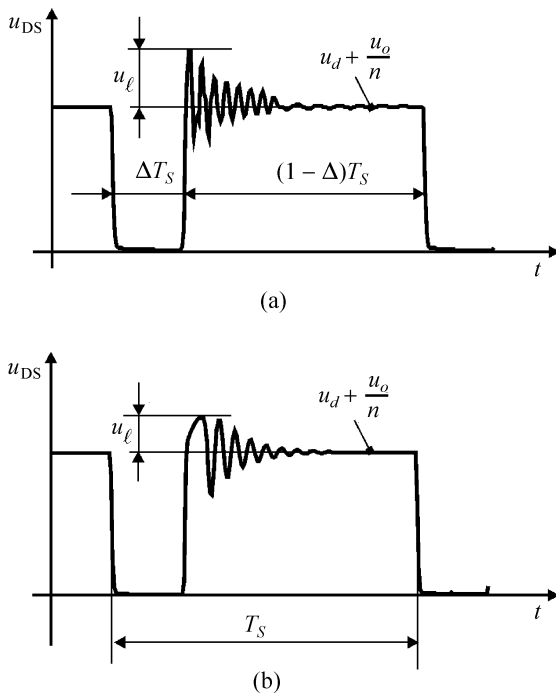


Fig. 2 (a) Transistor voltage, converter without clamp circuit, (b) Transistor voltage in converter with clamp circuit

### A. Dissipative RCD clamp circuit

Dissipative voltage clamp circuit is also shown in Figure 1. The clamp circuit consists of diode  $D_C$ , capacitor  $C_C$  and resistance  $R_C$ . Usually the clamp circuit provides a path for  $i_\ell$  to flow after the transistor has turned off. The energy stored in  $L_\ell$  is transferred to capacitor  $C_C$  and afterwards is dissipated by resistance  $R_C$ . By using proposed circuit the peak transistor voltage is clamped to the voltage, which is defined by next inequality:

$$u_d + u_C > u_d + \frac{u_o}{n}$$

where  $u_d$  is the dc supply voltage,  $u_C$  is the voltage across the clamp capacitor  $C_C$ ,  $u_o$  is the output voltage and  $n$  is transformer ratio. The clamp elements can be selected so that the  $C_C$  is large. In this case the voltage  $u_c(t)$  has no ripple:

$$C_C \gg \frac{T_s}{R_C} \quad (2)$$

where  $T_s$  is the switching period. This causes that:

$$u_C(t) = U_C. \quad (3)$$

The voltage  $U_C$  will rise until power dissipated by  $R_C$  is equal to average power transferred from  $L_\ell$ :

$$\frac{U_C^2}{R_C} = \frac{1}{2} L_\ell I^2 \frac{1}{T_s}. \quad (4)$$

The leakage inductance depends on winding geometry, and is not known until transformer is wound. This inductance can be measured by short circuit test, or can be estimate for a good, carefully wound transformer as:

$$L_\ell = 3\% \text{ of } L_m. \quad (5)$$

For RCD clamp elements design the energy stored in leakage inductance during  $0 \leq t \leq \Delta T_s$  can be estimated as:

$$W_\ell = \frac{1}{2} L_\ell I^2 \quad (6)$$

where  $\Delta$  is duty ratio. The average power transferred from inductance to clamp circuit is:

$$P_\ell = W_\ell \frac{1}{T_s}. \quad (7)$$

The transistor voltage ratio is usually known parameter. From (7) the dissipation on the clamp resistance  $R_C$  can be evaluated, and the voltage ( $U_{Rc}$ ) impressed on resistance during the switching off can be defined by next expression:

$$U_{Rc} = (1 - 0.25) U_{DS,max} - u_d \quad (8)$$

where  $U_{DS,max}$  represents the transistor voltage ratio. The resistance  $R_C$  can be evaluated by:

$$R_C = \frac{(U_{Rc})^2}{P_\ell}. \quad (9)$$

Clamp capacitor  $C_C$  can be evaluated by using (2). Figure 2 (b) shows the influence of the RCD clamp circuit. It is evident that the overshoot voltage is lower than in the case of the converter without RCD clamp circuit. Converter with all elements

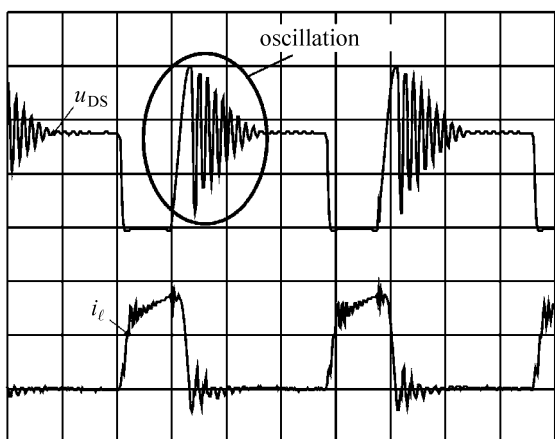


Fig. 3 Transistor voltage and current wave-shape (converter with RCD clamp circuit) experiment, x-axis 2  $\mu$ s/div,  $u_{DS}$ -axis 200 V/div,  $i_D$ -axis 2 A/div

was designed for output power of 200 W. In Figure 3 the experimental results of current and voltage measurement are shown. During the experiment the required output power has not been reached. Only the power level of 150 W has been reached due to the dissipation on the clamp diode caused by ringing oscillations. This undesirable mode of operation was further investigated more accurately by using SPICE simulator. The power stage was modeled and the simulation results, which are in good accordance with experiment, are shown in Figure 4.

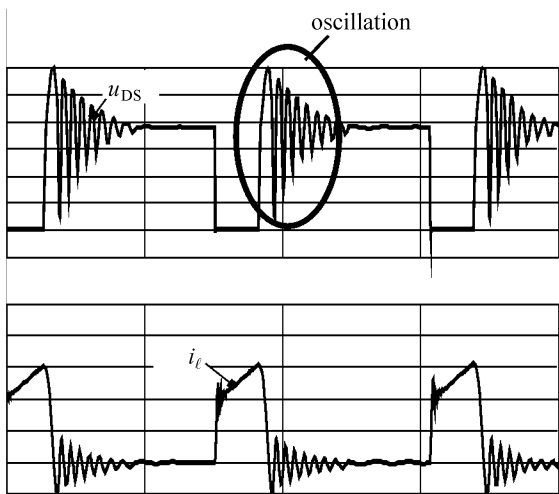


Fig. 4 Transistor voltage and current wave shape (converter with RCD clamp circuit) simulation, x-axis 5  $\mu$ s/div,  $u_{DS}$ -axis 100 V/div,  $i_D$ -axis 1 A/div

**B. Diode reverse recovery charge oscillation**

The ringing phenomena (oscillations) are indicated in Figures 3 and 4. The oscillation appears due to current stored in leakage inductance  $L_\ell$  and the

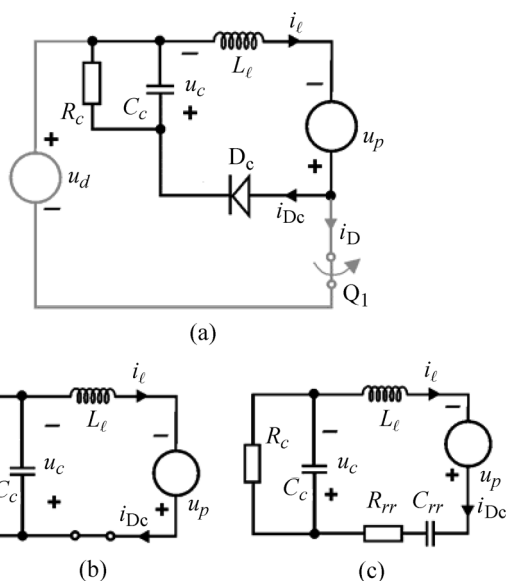


Fig. 5 All aspects of RCD clamp circuit

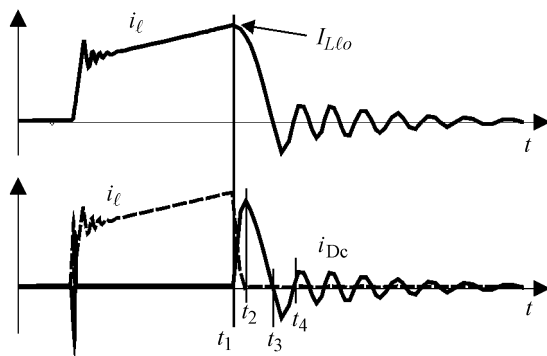


Fig. 6 The converter currents (with RCD clamp circuit), simulation

reverse recovery charge stored in junction capacitance of the clamp diode  $D_c$ . If switch  $Q_1$  is turned off, as it is indicated in Figure 5(a), the inductive current  $i_\ell$  is forced to flow through diode  $D_c$ . In the time interval  $t \in (t_1, t_2)$  the diode  $D_c$  and transistor  $Q_1$  commutates (Figure 6). This time interval is equivalent to the transistor switching-off time  $t_{off}$ . The voltage  $u_p$  (Figure 5) changed from  $u_d$  to  $-u_o/n$ . For  $t < t_1$  the voltage on  $C_c$  is zero due to the resistance  $R_c$  connected in parallel. The initial inductance current  $i_\ell$  after  $t > t_1$  is equal to the current at the end of  $Q_1$  switching-on interval ( $I_{Lto}$ ). Applying KVL around the loop in Figure 5 (b) gives:

$$\frac{d^2 i_\ell}{dt^2} + \frac{1}{R_c C_c} \frac{di_\ell}{dt} + \frac{1}{L_\ell C_c} i_\ell = \frac{1}{R_c L_\ell C_c} u_p \quad (10)$$

The characteristic equation of (10) dictates the character of the  $i_\ell$ . Due to the oscillatory response the roots are:

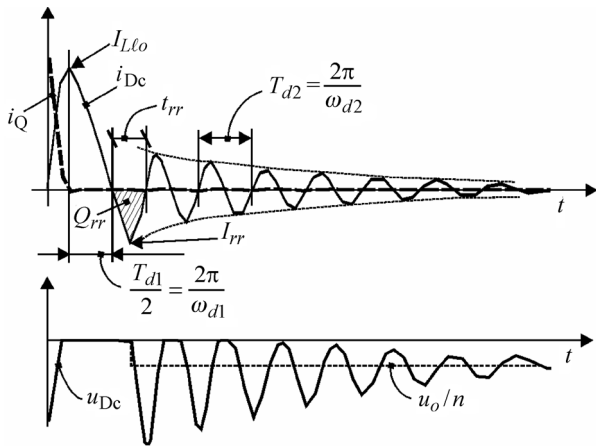


Fig. 7 The current damped oscillation (RCD clamp)

$$s_{1,2} = -\frac{1}{2R_c C_c} \pm \sqrt{\left(\frac{1}{2R_c C_c}\right)^2 - \frac{1}{L_c C_c}} = -\alpha_{c1} \pm \sqrt{\alpha_{c1}^2 - \omega_{o1}^2} = -\alpha_{c1} \pm j\omega_{d1} \quad (11)$$

where  $\alpha_{c1}$  is damping,  $\omega_{o1}$  is resonant frequency and  $\omega_{d1}$  is damped frequency. Considering the experimental and simulation results it is obvious that the response of the current  $i_\ell$  is damped and oscillatory in nature (Figure 7). At time  $t=t_3$  the diode current  $i_{Dc}$  through reaches zero. The interval  $T_{d1}/2$ , indicated in Figure 7, can be evaluated as:

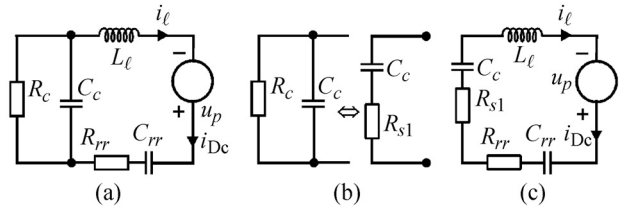
$$\frac{T_{d1}}{2} = \frac{2\pi}{\omega_{d1}} = \frac{2\pi}{\sqrt{\omega_o^2 - \alpha_c^2}}. \quad (12)$$

After  $t_3$  the diode switches-off and reverse-recovery process starts. In loop appears the reverse recovery charge of diode  $D_c$  (this charge is stored in nonlinear capacitor indicated as  $C_{rr}$ ) and due to the dissipation on the diode there is also the resistance  $R_{rr}$ . Unfortunately, the capacitor  $C_{rr}$  with the other elements in the loop (Figure 5(c)) establishes another oscillatory circuit. This oscillation causes additional dissipation on the resistance  $R_{rr}$ . In order to evaluate the oscillation parameters (Figure 5(c)) the parallel connection of  $R_c$ - $C_c$  combination has been transferred in series  $R_s$ - $C_c$  combination by using criteria of the equal current as it is shown in Figure 8. Applying KVL around the loop in Figure 8(c) gives:

$$\frac{d^2 i_\ell}{dt^2} + \frac{R_s}{L_\ell} \frac{di_\ell}{dt} + \frac{C_c + C_{rr}}{L_\ell C_{rr} C_c} i_\ell = 0 \quad (13)$$

where resistance  $R_s$  is evaluated by:

$$R_s = R_{rr} + R_{s1} = R_{rr} + \frac{R_c}{1 + \omega_{o2}^2 R_c^2 C_c^2}.$$


 Fig. 8  $R_s$  evaluation

This resistance  $R_s$  depends on frequency that could be evaluated as indicated below in (15). Capacitance  $C_{rr}$  can be evaluated from Figure 9 as it follows from [6]. The forward voltage  $U_{on,diode}$  is impressed on diode until current through diode reaches  $I_{rr}$  (Figure 10). During this time interval, this is cca.  $t_{rr}/2$ , in the diode capacitance is stored half of reverse recovery charge  $Q_{rr}$ .

$$Q_{rr} = \frac{1}{2} \frac{I_{rr} t_{rr}}{2} \quad \text{and} \quad U_{on,diode} = \frac{Q_{rr}}{2C_{rr}}$$

and finally:

$$C_{rr} = \frac{Q_{rr}}{2U_{on,diode}} = \frac{Q_{rr}}{1.4}. \quad (14)$$

The characteristic equation of (13) dictates the character of the  $i_\ell$ . Due to oscillatory response the roots are:

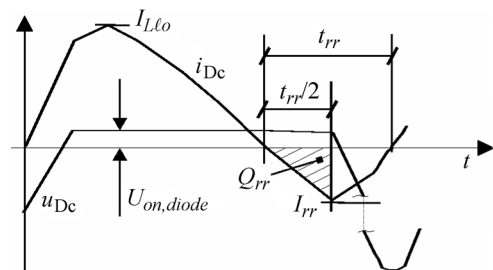
$$s_{1,2} = -\frac{R_s}{2L_\ell} \pm \sqrt{\left(\frac{R_s}{2L_\ell}\right)^2 + \frac{C_c + C_{rr}}{L_\ell C_{rr} C_c}} = -\alpha_{c2} \pm \sqrt{\alpha_{c2}^2 - \omega_{o2}^2} = -\alpha_{c2} \pm j\omega_{d2}. \quad (15)$$

According to (15) the period of damped oscillation process indicated in Figure 8 is:

$$T_{d2} = \frac{2\pi}{\omega_{d2}} = \frac{2\pi}{\sqrt{\alpha_{c2}^2 - \omega_{o2}^2}} \quad (16)$$

and the damped frequency  $\omega_{d2}$  is:

$$\omega_{d2} = \sqrt{\left(\frac{R_s}{2L_\ell}\right)^2 + \frac{C_c + C_{rr}}{L_\ell C_{rr} C_c}}. \quad (17)$$


 Fig. 9 The diode  $D_c$  switching-off

The diode current and voltage oscillate as it is shown in Figure 7. This oscillation appears in the reverse conducting mode of the diode  $D_c$ . If the temperature of the diode exceeds its thermal rating, the diode fails.

The diode dissipation  $P_{AVG,diode}$  was evaluated by SPICE, and in the case of chosen converter was cca. 20W when the 150W output load was applied. This dissipation requires additional cool sink or some other preventive measure as it is RC-RCD clamp circuit.

### 3 DISSIPATIVE RC-RCD CLAMP CIRCUITS

In previous section was shown that the oscillatory process (due to reverse recovery capacitance  $C_{rr}$ ) provokes additional dissipation on the clamp diode. This oscillatory process can be damped by using an additional RC snubber circuit as it is shown in Figure 10. Therefore whole clamp circuit has RC-RCD structure. Due to the different damped frequencies  $\omega_{d1}$  and  $\omega_{d2}$ , the resistance  $R_c$  is not capable to damp the oscillatory process provoked by diode capacitance  $C_{rr}$ .

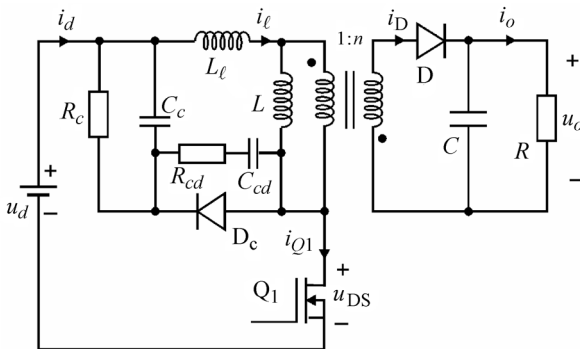


Fig. 10 Dissipative RC-RCD clamp circuit in flyback converter

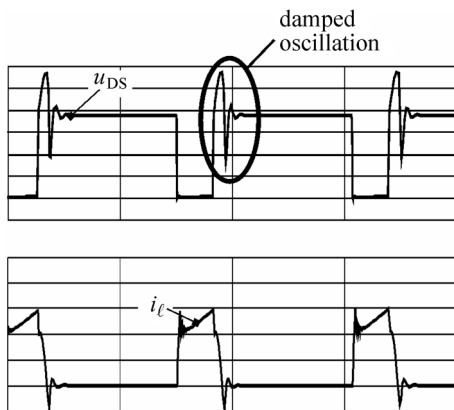


Fig. 11 Transistor voltage and current wave shape (converter with RC-RCD clamp circuit) simulation, x-axis 5  $\mu$ s/div,  $u_{DS}$ -axis 100 V/div,  $i_L$ -axis 1 A/div

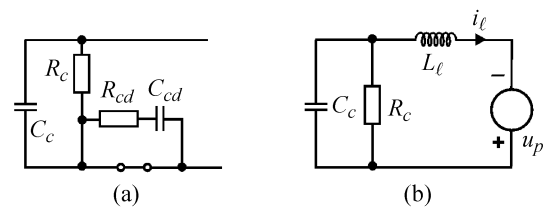


Fig. 12 All aspects of RC-RCD clamp circuit

This process was first investigated by SPICE. The results are shown in Figure 11. Figure 12 shows all aspects of RC-RCD circuit when  $Q_1$  is turned-off. As follows from Figure 12(a) the diode snubber combination  $R_{cd}-C_{cd}$  is short connected and does not have impact on current while diode is turned-on. The transient response of the current is exactly the same as it is indicated by (10). The diode current reaches zero point at the time instant  $t_3$  as it is shown in Figure 14. The transient response does not differ as in the case of the ordinary RCD clamp circuit.

$$t_3 - t_2 = \frac{T_{d1}}{2} = \frac{2\pi}{\omega_{d1}} = \frac{2\pi}{\sqrt{\omega_{o1}^2 - \alpha_{c1}^2}} \quad (18)$$

After  $t_3$  the diode switches-off and reverses recovery process starts. The oscillation caused by capacitor  $C_{rr}$  can be damped by appropriate combination of  $R_{cd}-C_{cd}$ . This process is shown in Figures 14 and 15. In order to estimate transient response when  $R_{cd}-C_{cd}$  snubber operates, the situation shown in Figure 13 (a) must be considered. In first step the element of partial equivalent circuit can be evaluated by using transformation, which series  $R_{cd}-C_{cd}$  and  $C_{rr}-R_{rr}$  combinations transfer in parallel  $R_{pcd}-C_{cd}$  and  $C_{rr}-R_{pr}$  combinations by using criteria of the equal dissipation as it is shown in Figure 13(c). Resistance  $R_{pcd}$  and  $R_{pr}$  are evaluated by:

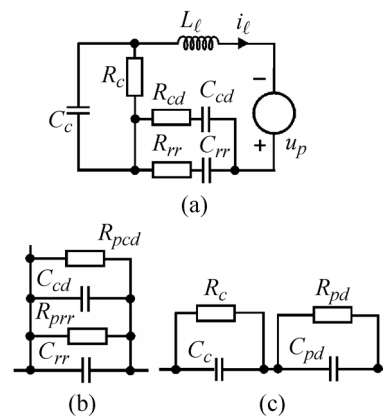


Fig. 13 All aspects of RC-RCD clamp circuit

$$R_{pcd} = R_{cd} + \frac{1}{R_{cd}} \frac{1}{\omega_{o3}^2 C_{cd}^2},$$

and

$$R_{pr} = R_{rr} + \frac{1}{R_{rr}} \frac{1}{\omega_{o3}^2 C_{rr}^2}.$$

and further:

$$R_{pd} = R_{pcd} // R_{pr} \quad \text{and} \quad C_{pd} = C_{cd} + C_{rr}.$$

In order to study the circuit shown in Figure 13(c) additional transformation (equal current criteria) is needed. This transformation is indicated in Figure 16. The equivalent resistances are:

$$R_{sc} = \frac{R_C}{1 + \omega_{o3}^2 R_C^2 C_C^2}, \quad R_{sd} = \frac{R_{pd}}{1 + \omega_{o3}^2 R_{pd}^2 C_{pd}^2}.$$

The frequency  $\omega_{o3}$  is natural frequency of the equivalent circuit and it will be explained below. The current  $i_\ell$  is described by second order equation:

$$\frac{d^2 i_\ell}{dt^2} + \frac{R_{eq}}{L_\ell} \frac{di_\ell}{dt} + \frac{C_c + C_{pd}}{L_\ell C_{pd} C_c} i_\ell = 0. \quad (19)$$

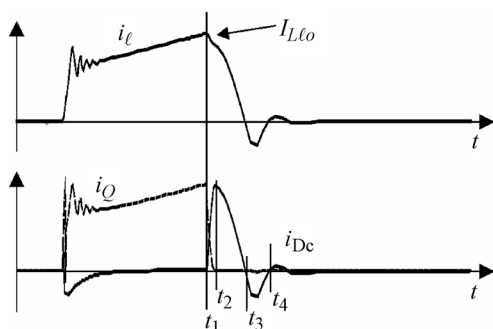


Fig. 14 The converter currents (with RC-RCD clamp circuit), simulation

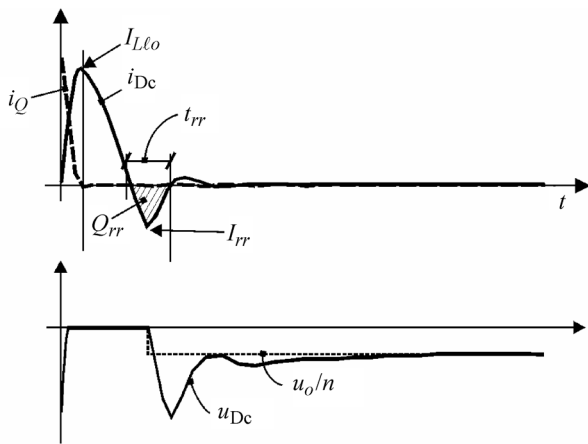


Fig. 15 The current damped oscillation (RCD clamp)

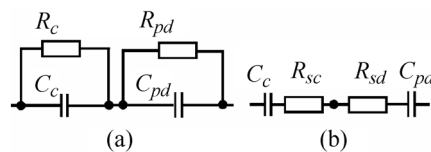


Fig. 16 The RC-RCD equivalent circuits

where  $R_{eq} = R_{sc} + R_{sd}$ . The characteristic equation of (19) dictates the character of the  $i_\ell$ . The roots are:

$$s_{1,2} = -\frac{R_{eq}}{2L_\ell} \pm \sqrt{\left(\frac{R_{eq}}{2L_\ell}\right)^2 - \frac{C_c + C_{pd}}{L_\ell C_{pd} C_c}} = -\alpha_{c3} \pm \sqrt{\alpha_{c3}^2 - \omega_{o3}^2} \quad (20)$$

where:

$$\alpha_{c3} = \frac{R_{eq}}{2L_\ell}. \quad (21)$$

In order to avoid the undesired oscillation the damping of the process must satisfy inequality:

$$\left(\frac{R_{eq}}{2L_\ell}\right)^2 \geq \omega_{o3}^2 = \frac{C_c + C_{pd}}{L_\ell C_{pd} C_c}. \quad (22)$$

From equality (21) and inequality (22) the  $R_{cd}$  and  $C_{cd}$  can be evaluated. From the well known response of second order system the low damping allows the oscillation to continue and too much damping results in high resistor power dissipation. So reasonable damping for  $\alpha_{o3}$  is 0.5. By using this procedure the diode snubber elements  $R_{cd}$  and  $C_{cd}$  have been designed. Figure 17 shows the experimental result. The power dissipation on the diode has been decreased significantly.

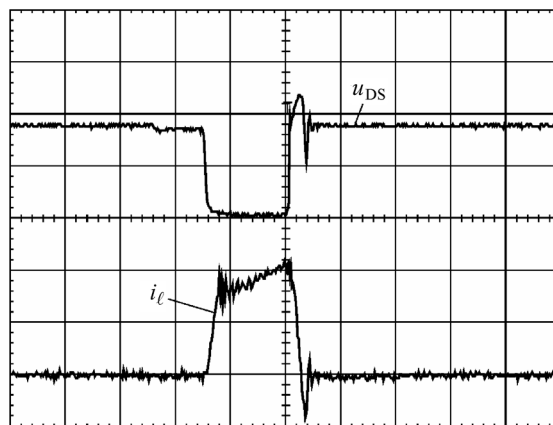


Fig. 17 Transistor voltage and current wave shape (converter with RC-RCD clamp circuit) experiment, x-axis 2  $\mu$ s/div,  $u_{DS}$ -axis 200 V/div,  $i_D$ -axis 2 A/div

#### 4 CONCLUSION

The flyback converter of 200 W output power has been tested. The converter operated with the frequency of 140 kHz. Oscillatory process called »ringing« occurs in flyback converter when the clamp diode is just turning-off. Due to this oscillation the diode thermal rating has been violated. By using the RC-RCD clamp circuit this thermal effect can be neglected and the power rating of the converter can be improved. The power rating increased from 150 W with RCD clamp circuit to the 200 W with RC-RCD clamp circuit. This clamp circuit is capable to improve the EMC as well.

#### REFERENCES

- [1] W. McMurray, **Selection of Snubbers and Clamps to Optimize the Design of Transistor Switching Converters**. IEEE Transaction on Ind. Application, vol. IA-16, pp. 513–523, July-Avg. 1980.
- [2] T. Ninomiya, T. Tanaka, K. Harada, **Analysis and Optimization of a Nondissipative LC Turn-off Snubber**. IEEE Transaction on Power Electronics, vol. 3, No. 2, pp. 147–156, April 1988.
- [3] F. Z. Peng, G. Su, L. M. Tolbert, **A Passive Soft Switching Snubber for PWM Inverters**. IEEE Transaction on Power Electronics, vol. 19, No. 2, pp. 363–370, March 2004.
- [4] C. Ji, M. K. Smith, K. M. Smedely, **Cross Regulation of Flyback Converters Solutions**. IECON 1991: IEEE, October, 1991, pp. 319–330.
- [5] R. W. Ericson, D. Maksimovic, **Fundamentals of Power Electronics**. Kluwer Academic Publisher, 2001.
- [6] N. Mohan, T. M. Undeland, W. P. Robbins, **Power Electronics: Converters, Application and Design**. John Wiley & Sons, New York, 1976.

**Smanjenje gubitaka istitravanja kod neizravnog istosmjernog pretvarača s transformatorom uporabom RC-RCD prigušnog člana.** Neizravni istosmjerni pretvarač s transformatorom jedan je od najpopularnijih istosmjernih pretvarača za izvore napajanja malih snaga. Zbog rasipnog induktiviteta transformatora tijekom rada pretvarača dolazi do pojave prenapona, koji se mogu ograničiti pomoću disipativnih RCD ili nedisipativnih LCD prigušnih sklopova. Oba prigušna sklopa sadrže diodu. Reverzni naboj oporavljanja diode uzrokuje oscilacije koje uzrokuju dodatne gubitke u prigušnom sklopu. Članak opisuje pojavu istitravanja i uporabu RC-RCD prigušnog sklopa za prigušenje oscilacija uzrokovanih prigušnom diodom. Opisani prigušni sklop omogućava povećanje djelotvornosti neizravnog istosmjernog pretvarača s transformatorom.

**Ključne riječi:** gubici istitravanja, neizravni istosmjerni pretvarač s transformatorom, prigušni sklop

#### AUTHORS' ADDRESSES

**M. Milanović**<sup>1,2)</sup>

**J. Korelič**<sup>1)</sup>

**A. Hren**<sup>1)</sup>

**F. Mihalič**<sup>1)</sup>

**P. Šlibar**<sup>2)</sup>

<sup>1)</sup> University of Maribor, FERl, Maribor, Slovenia

<sup>2)</sup> TECES, Development centre for electrical machines  
Maribor, Slovenia

Received: 2006-03-30